AEM
Journals.ASM.org

Exposure to Solute Stress Affects Genome-Wide Expression but Not the Polycyclic Aromatic Hydrocarbon-Degrading Activity of *Sphingomonas* sp. Strain LH128 in Biofilms

Tekle Tafese Fida,[a] Philip Breugelmans,[a] Rob Lavigne,[b] Edith Coronado,[c] David R. Johnson,[c] Jan Roelof van der Meer,[c] Antonia P. Mayer,[c] Hermann J. Heipieper,[d] Johan Hofkens,[e] and Dirk Springael[a]

Division of Soil and Water Management, KU Leuven, Heverlee, Belgium[a]; Division of Gene Technology, KU Leuven, Heverlee, Belgium[b]; Departement of Fundamental Microbiology, University of Lausanne, Lausanne, Switzerland[c]; Department Environmental Biotechnology, Helmholtz Centre for Environmental Research–UFZ, Leipzig, Germany[d]; and Department of Chemistry, KU Leuven, Heverlee, Belgium[e]

Members of the genus *Sphingomonas* are important catalysts for removal of polycyclic aromatic hydrocarbons (PAHs) in soil, but their activity can be affected by various stress factors. This study examines the physiological and genome-wide transcription response of the phenanthrene-degrading *Sphingomonas* sp. strain LH128 in biofilms to solute stress (invoked by 450 mM NaCl solution), either as an acute (4-h) or a chronic (3-day) exposure. The degree of membrane fatty acid saturation was increased as a response to chronic stress. Oxygen consumption in the biofilms and phenanthrene mineralization activities of biofilm cells were, however, not significantly affected after imposing either acute or chronic stress. This finding was in agreement with the transcriptomic data, since genes involved in PAH degradation were not differentially expressed in stressed conditions compared to nonstressed conditions. The transcriptomic data suggest that LH128 adapts to NaCl stress by (i) increasing the expression of genes coping with osmolytic and ionic stress such as biosynthesis of compatible solutes and regulation of ion homeostasis, (ii) increasing the expression of genes involved in general stress response, (iii) changing the expression of general and specific regulatory functions, and (iv) decreasing the expression of protein synthesis such as proteins involved in motility. Differences in gene expression between cells under acute and chronic stress suggest that LH128 goes through changes in genome-wide expression to fully adapt to NaCl stress, without significantly changing phenanthrene degrading activity.

Polycyclic aromatic hydrocarbons (PAHs) are persistent environmental contaminants in soil (37). Despite their low bioavailability, microbial degradation is a major process for PAH removal in soil, either through indigenous microorganisms or through bioaugmentation (37). One important bacterial genus implicated in aerobic PAH biodegradation in soil is *Sphingomonas*. Members of this genus are often isolated as PAH degraders from PAH-contaminated environments and are ubiquitous in soil, water, and sediments (2, 39). In addition, they can degrade many other xenobiotics (62).

In terrestrial habitats, bacteria often colonize soil particles and plant surfaces as biofilms or microcolonies (21). Biofilm cells show advantages over planktonic cells toward environmental stress, such as an increased tolerance to antibiotics and biocides (6). Moreover, PAH degraders often grow as biofilms on or near PAH sources, which is hypothesized to be a mechanism for increasing PAH substrate transfer toward the cell (37). Bacteria in soil are subjected to various environmental stresses due to fluctuations in environmental conditions, which in turn can affect bacterial survival and activities including organic pollutant degradation. One of the most important stress factors in soil is the water potential (46). An important component of the soil water potential is the solute content (46), since changes in solute content affect cell turgor pressure and result in cellular osmotic stress and eventually ionic stress (52). Changes in solute content occur regularly in soil due to periodical weather-bound drought-wet cycles and the input of anthropogenic solutes from industrial and agricultural activities such as irrigation with poor quality water and the use of salt for deicing roads (43, 48). The latter results in increased sodium chloride concentrations in topsoil in urban environments and near highways that can also contain significant PAH concentrations (36, 48). Also, uptake of water by plants can result in a local increase in solute concentration around the plant roots (43), which can affect rhizoremediation activities (40).

To minimize the effect of a solute stress, microorganisms display a number of cellular responses, such as the adjustment of intracellular osmolyte concentrations by the accumulation of compatible solutes (12, 61) and adjustment of the degree of membrane fatty acid *cis-trans* isomerization and saturation (27). Studies on cellular responses on solute stress in bacteria emphasized on enterobacteria such as *Escherichia coli* (51) and on *Pseudomonas aeruginosa* (1). Few reports exist on soil bacteria and xenobiotic compound-degrading bacteria (22, 27), although such studies are important for understanding the natural attenuation of xenobiotics in soil and for optimizing soil bioremediation activities. In addition, reported studies on solute stress response by pollutant-degrading bacteria did not assess the response of the organisms when actively degrading and growing on the pollutant itself. Neither do they address the fact that in soil, bacteria are often present as aggregated sessile communities attached as biofilms to soil particles (54).

Received 14 August 2012 **Accepted** 13 September 2012
Published ahead of print 21 September 2012
Address correspondence to Dirk Springael, dirk.springael@ees.kuleuven.be.
Supplemental material for this article may be found at http://aem.asm.org/.

doi:10.1128/AEM.02516-12

We examine here the physiological and transcriptomic response of biofilms of the PAH-degrading *Sphingomonas* sp. strain LH128 on solute stress when degrading phenanthrene. For this purpose, strain LH128 was grown in continuous flow chambers that contain solid phenanthrene as a sole carbon source and that allow easy recovery of biofilm cells for transcriptomic and physiological analysis. As in other studies addressing the bacterial response to solute stress, NaCl was used as the osmolyte (9, 38). Both acute and chronic solute stress was invoked to assess differences in short-term and long-term responses.

MATERIALS AND METHODS

Bacterial strain and growth conditions. *Sphingomonas* sp. LH128 uses phenanthrene as the sole source of carbon and energy (2). In the present study, a green fluorescent protein (GFP)-tagged derivative of LH128 was used (63). For all experiments, LH128 was precultured at 27°C in 25 ml of R2A medium and harvested in the exponential growth phase (optical density at 600 nm [OD_{600}] of 0.6). The cells were centrifuged at 5,000 × *g* for 10 min in a Becton Dickinson centrifuge (Benelux, Netherlands), washed twice with 0.9% saline solution, and suspended in a defined phosphate-buffered minimal medium (MM) at an OD_{600} of 0.25 (2.4×10^7 cells per ml). The compositions of R2A and MM were as reported previously (50, 59).

Growth in suspended batch cultures. The effect of the NaCl concentration on growth of strain LH128 on glucose was assessed in triplicate in suspended batch cultures in 25-ml test tubes. The tubes contained 7.2 ml of MM with 2 g of glucose $liter^{-1}$ and increasing concentrations of NaCl (50, 150, 300, 450, and 600 mM) and were inoculated with LH128 cells at a final density of 2.4×10^7 cells per ml. Growth was monitored by determining the OD_{600}, and growth rates were determined from the slopes of the growth curves.

Cultivation of LH128 biofilms in flow chambers. LH128 biofilms were grown in glass flow chambers (exterior sizes of 85 by 60 by 10 mm, total interior volume of ~45 ml) equipped with one inlet and three outlets (see Fig. S1 in the supplemental material). Silicone tubing with 1.5-mm internal diameter was connected to the inlets and outlets, and the flow chambers were autoclaved twice. Glass slides (75 by 25 by 1 mm) were coated with 12.5 mg per slide of phenanthrene dissolved in acetone at a concentration of 50 mg ml^{-1}. The acetone was allowed to evaporate in a laminar flow, and two coated slides were aseptically positioned in each chamber. The flow chambers were covered with Viton rubber, glued with silicone, and irrigated with MM at a flow rate of 60 ml h^{-1} using a Watson-Marlow 205S/CA multichannel peristaltic pump (Watson-Malow NV, Belgium) until the chambers were completely filled. The flow chambers were inoculated by stopping the flow, clamping off the inlet and outlet tubes, and injecting 2 ml of a LH128 suspension (prepared as reported above) using a 1-ml plastic insulin syringe with needle (Terumo, Europe NV, Belgium). The cells were allowed to attach to the glass slides for 1 h, after which the MM was supplied continuously at a rate of 15 ml h^{-1} creating dilution rates of around 0.3 h^{-1}. Biofilms were grown at 25°C for a total of 11 days and then analyzed. This time point was chosen based on preliminary experiments that defined 11 days as the minimum time needed for acquiring sufficient biomass for transcriptome analysis without depletion of phenanthrene in the flow chamber. Conditions of solute stress were imposed by irrigating the flow chambers with MM containing 450 mM NaCl at a rate of 15 ml h^{-1} from day 8 for a period of 3 days (chronic stress condition) or at day 11 for 4 h (acute stress condition). Simultaneously, biofilm systems without stress were operated (control condition). Uninoculated chambers were similarly operated for 11 days as a cell-free control. For each condition, three replicate flow chambers were operated. At day 11, the flow chambers were opened and from each replicate chamber, one glass slide was removed for confocal laser scanning microscopy (CLSM) analysis, and one was removed for transcriptomic analysis. In an identical but separate triplicate experiment, one glass slide was used for fatty acid methyl ester (FAME) analysis, and the other was used for determining [^{14}C]phenanthrene mineralization activity.

Oxygen consumption. Oxygen consumption in the biofilm systems was determined by measuring the concentrations in the influent and effluent of the flow chambers using a Unisense oxygen microsensor electrode (Unisence A/S, Aarhus N, Denmark). For calibration, the sensor tip was placed in water, bubbled with oxygen-saturated air, and then transferred into an anoxic solution consisting of 0.1 M sodium ascorbate and 0.1 M NaOH. Signals were recorded in millivolts and converted to oxygen concentration (in μM) by using Unisence SensorTrace Pro v2.0 software. Samples were taken from the influent and effluent by means of 10-ml syringes with hypodermic needles flushed with oxygen-free nitrogen gas. The sensor was immediately immersed into the sample inside the syringes and oxygen concentrations recorded. A two-tailed Student *t* test with a *P* value cutoff of 0.05 was used to test for significance of differences in oxygen consumption between stressed and nonstressed biofilms.

CLSM analysis of biofilms. Glass slides removed from the flow chambers were washed carefully by immersing in MM to remove planktonic cells. For each condition, the biofilm present in each of the three replicate flow chambers was analyzed on an Olympus IX81 inverted microscope equipped with a Fluoview FV1000 confocal scanning unit and two lasers. The green fluorescent protein (GFP) signal of LH128 was collected from five different locations along the glass slide by excitation with a 488-nm laser line in combination with a 505- to 540-nm band-pass emission filter. Phenanthrene crystals, which emit blue fluorescence, were visualized by a 375-nm laser line excitation in combination with a 430- to 470-nm band-pass emission filter. Images were captured at 1.5-μm increments with a ×20/0.75 objective lens (Olympus). Fluorescence projections and sections through the images were generated using the IMARIS software package (Bitplane AG, Zurich, Switzerland). Quantification of biomass (biovolume) from a minimum of five different images per microscopic glass slide was performed using COMSTAT image-processing software (28) using a script written in MATLAB (MathWorks, Natick, MA). A two-tailed Student *t* test with a *P* value cutoff of 0.05 was used to test for significant differences in biomass between stressed and nonstressed biofilms.

FAME analysis of biofilms. FAME analysis was performed on biofilms cells recovered from each of the three replicate flow chamber of each condition. After the biofilm was scraped off the glass slide, the phenanthrene crystals were allowed to settle, and the recovered cells were centrifuged at 3,000 × *g* for 10 min in a Becton Dickinson centrifuge. The cells were resuspended in 0.5 ml of water, after which the fatty acids were directly extracted using methanol-chloroform as described previously (7). The fatty acids were converted into FAMEs, and the FAMEs were identified and quantified by gas chromatography-quadrupole mass spectrometry, as described previously (27). The degree of saturation of membrane fatty acid was defined as the ratio between the sum of the relative proportions of palmitic acid (16:0) and stearic acid (18:0) divided by the sum of the relative proportions of palmitoleic acid (16:1Δ9*cis*) and *cis*-vaccenic acid (18:1Δ11*cis*). These four fatty acids compose >95% of the bacterial membrane fatty acids. A two-tailed Student *t* test with a *P* value cutoff of 0.05 was used to test whether the degree of saturation was significantly different between FAME composition for control biofilms and for biofilms exposed to solute stress.

[^{14}C]phenanthrene mineralization activity of biofilm cells. The phenanthrene mineralization activity of biofilm cells was examined as described previously (59) by measuring the production of $^{14}CO_2$ from 9-^{14}C-labeled phenanthrene (Sigma; 13.1 mCi $mmol^{-1}$, dissolved in methanol; radiochemical purity, 98.9%) in 15-ml Pyrex tubes containing 4.5 ml of MM with 120 kBq of ^{14}C-labeled phenanthrene ml^{-1} (final phenanthrene concentration of 0.012 mg $liter^{-1}$) and inoculated with biofilm cells. The assay was performed in triplicate for each of the three replicate flow chambers of each condition. Biofilms cells were scraped off from the glass slides using a scalpel blade while flushing with MM. After the phenanthrene crystals were settled, viable cells producing GFP were

counted in a Helber counting chamber by epifluorescence microscopy. A 0.5-ml portion of the cell suspension (2.4×10^5 cells) was added to the Pyrex tubes, which were then closed with Teflon-lined stoppers equipped with glass vials containing 1 ml of 0.5 M NaOH, to trap $^{14}CO_2$, followed by incubation at 20°C on a rotary shaker at 150 rpm. Trapped $^{14}CO_2$ was measured in a liquid scintillation counter (Packard Tri-Carb 1600CA; Perkin-Elmer) after 4 and 16 h of incubation, as described previously (59). A two-tailed Student *t* test with a *P* value cutoff of 0.05 was used to test for significant differences between stressed and nonstressed cells.

RNA extraction from biofilms. RNA was separately extracted from each of the three replicate flow chambers of each condition. Glass slides containing biofilms were carefully removed from the flow chambers and washed by immersion in MM containing RNAprotect bacterial reagent (Qiagen, Benelux BV) to remove planktonic cells and to stabilize the RNA. Biofilm cells, together with the phenanthrene crystals, were then scraped off from the glass slides using a sterile scalpel blade while flushing with 2 ml of MM containing 1 ml of fresh RNAprotect bacterial reagent. RNA was immediately extracted using a Promega SV total RNA extraction kit (Promega, Benelux BV) with minor modifications of the protocol (centrifugation was performed at 17,000 × *g* instead of at 14,000 × *g* and 200 μl of Tris-EDTA containing lysozyme was used instead of 100 μl). The RNA was eluted with 80 μl of RNase-free water and precipitated to the required concentration after adding 0.1 volume of 3 M sodium acetate and 2 volumes of 100% ethanol. Traces of remaining DNA were removed by using the Turbo DNA-free kit (Ambion), and its absence was verified by performing PCR using degenerate primers (DOF1, AARGGYTTCATYTTCGGY TGC; DOR1, TGSGTCCAKCCSACRTGAT) targeting *phnA1f*. The integrity and purity of the RNA extracts were checked by using a Bioanalyzer 2100 (Agilent Technologies).

Genome sequence and design of microarray probes. A draft sequence of the genome of *Sphingomonas* sp. LH128 was obtained using Illumina (Solexa) sequencing (Baseclear Labservices, Leiden, Netherlands). The draft sequence consisted of 659 contigs, which were concatenated using a 45-base linker sequence (CATNCATNCATNTAGNTAGN TAGCTANCTANCTAATGNATGNATG) that provided start and stop codons in six frames for truncated open reading frames (ORFs) at the termini of the contigs. The concatenated contigs were submitted to the GeneMark ORF prediction software (5) as one Fasta file. About 7,275 ORFs were predicted and a Greengene batch BLAST search was run against the NCBI database to predict the gene functions encoded by ORFs. Microarray probes were designed for the obtained ORFs using YODA (Yet Another Oligonucleotide Design Application) software (45). A total of 12,663 60-mer probes were designed which targeted >96% of the predicted ORFs (7,033 of 7,275). About 86% of the probes were designed with stringent parameters: one to two nonoverlapping probes per gene, a maximum of 70% identity to nontarget sequences, a maximum of 15 consecutive matches to nontarget sequences, a melting temperature range of 6°C from the average, a GC content range of 12% from the average, and a maximum of four consecutive polynucleotides. The remaining 10% of the probes were designed with the following nonstringent parameters: one to two nonoverlapping probes per gene, a maximum of 80% identity to nontarget sequences, a maximum of 15 consecutive matches to nontarget sequences, a melting temperature range of 15 to 20°C, a GC content range of 15 to 25%, and a maximum of four consecutive polynucleotides. Twenty control probes were also included in the design as an internal quality control and to assess reproducibility (see Table S1 in the supplemental material). The probes were submitted online to the Agilent Custom Array and printed on a 8×15,000 array platform (eight arrays per slide; 15,000 probes per array) using the Agilent Technology format.

Nucleic acid labeling. The nucleic acids were labeled with cyanine 3-labeled dCTP while reverse transcribing the RNA to cDNA using a one-color gene expression protocol of Agilent Technologies with some modifications. Briefly, the reaction was performed in 25 μl containing 4 μg of RNA, 10 mM each dATP, dGTP, and dTTP, 5 mM unlabeled dCTP, 200 U of Superscript II reverse transcriptase (Invitrogen), 625 ng of random hexanucleotide primer (Promega), and 1.25 mM cyanine 3-labeled dCTP (Perkin-Elmer). Reactions were performed at 42°C for 2 h, followed by 70°C for 10 min. Residual RNA was removed by alkaline hydrolysis using 100 mM NaOH and heating at 65°C for 20 min, followed by neutralization using 100 mM HCl and 300 mM sodium acetate (pH 5.2). The labeled cDNA was purified using a MiniElute PCR purification kit (Qiagen). The quality of the labeled cDNA and the cyanine 3-labeled dCTP incorporation efficiency was assessed using the microarray function of the NanoDrop spectrophotometer.

Microarray analysis. Microarray analysis was done separately for each of the three replicate biofilms of each condition with one array per replicate RNA and was performed according to the "minimum information about a microarray experiment" (MIAME) procedure (8). A total of 60 ng of labeled cDNA with an incorporation efficiency of cyanine 3-labeled dCTP of between 3 and 5.9% was hybridized with the array for 17 h at 65°C. The array was washed and scanned according to the one-color microarray-based gene expression analysis protocol of Agilent Technologies. The Agilent Feature Extraction software package (version 9.5.3; Agilent Technologies) was used to extract the hybridization signal intensities from the scanned images. Normalization of the signal intensities (quantile normalization) and analysis of the data were done using the GeneSpring GX software package (version 11; Agilent technologies). To test for significantly differentially expressed genes, Welch's *t* test with unequal variances was first used to calculate *P* values, followed by the Benjamini-Hochberg procedure to correct the *P* values for multiple hypothesis testing and convert the *P* values into false discovery rates (FDRs) (4). Genes with significant differential expression between conditions were defined as having an FDR of <0.05 and a fold difference in hybridization signal intensity of ≥2. GeneSpring analysis included a hierarchical clustering and principal component analysis (PCA) to test the reproducibility of samples.

RT-qPCR. Reverse transcription real-time quantitative PCR (RT-qPCR) targeting selected transcripts was performed on RNA recovered from each of the three replicate flow chambers of each condition. RNA (500 ng) that had been used in the microarray analysis was converted to cDNA using random hexamers and Superscript II reverse transcriptase (Invitrogen). The resulting cDNA was used in real-time PCR using a SYBR green RT-qPCR kit (Westburg, Leusden, Netherlands) and gene-specific primers to quantify the transcript numbers of selected genes in a Rotor-Gene RG-3000 real-time PCR cycler (Westburg). Primers were designed using FastPCR software (PrimerDigital, Ltd., Helsinki, Finland) or by visual inspection of the target gene sequences, and the specificity was checked by BLAST analysis. The PCR conditions were as follows: an initial hold temperature of 95°C for 15 min, followed by 40 cycles of denaturation at 95°C for 5 s, annealing at 50 to 56°C for 5 s (depending on the primers used), and elongation at 72°C for 15 s, with a final hold temperature of 72°C for 10 min. The primer sequences and the applied annealing temperatures to amplify the selected genes are given in Table S2 in the supplemental material. Calibration curves were performed with cDNA of target genes amplified by PCR and serially diluted over a range of 7 to 10 orders of magnitude after purification. The RNA transcript copy number was normalized to the total amount of transcript quantified using a NanoDrop spectrophotometer. The ratio of transcript copy number per mass of RNA obtained from stressed biofilms to transcript copy number per mass of RNA obtained from nonstressed biofilms was calculated for each of the applied stress conditions.

Microarray data accession number. The microarray data discussed here have been deposited in NCBI's Gene Expression Omnibus (18) and are accessible under GEO series accession number GSE38296.

RESULTS

Effect of solute stress on LH128 growth on glucose in suspended batch cultures. The effect of increasing concentrations of NaCl on the growth of LH128 on glucose was examined in suspended batch cultures to select an appropriate concentration of NaCl to be ap-

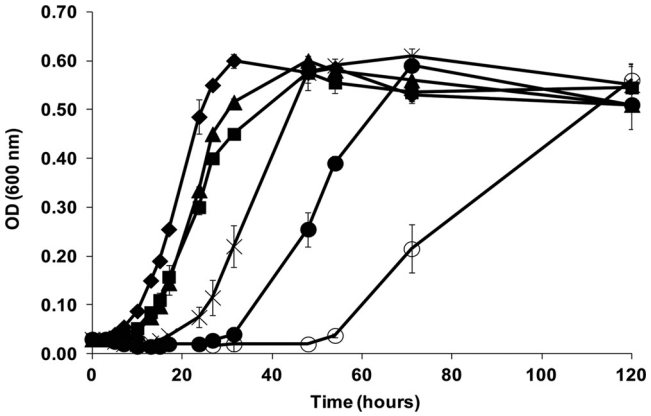

FIG 1 Growth of *Sphingomonas* sp. LH128 in MM with glucose in the presence of increasing concentrations of NaCl, indicated as follows: control (◆), 50 mM NaCl (■), 150 mM NaCl (▲), 300 mM NaCl (×), 450 mM NaCl (●), and 600 mM NaCl (○). The values shown are the average of three biological replicates with the indicated standard deviations.

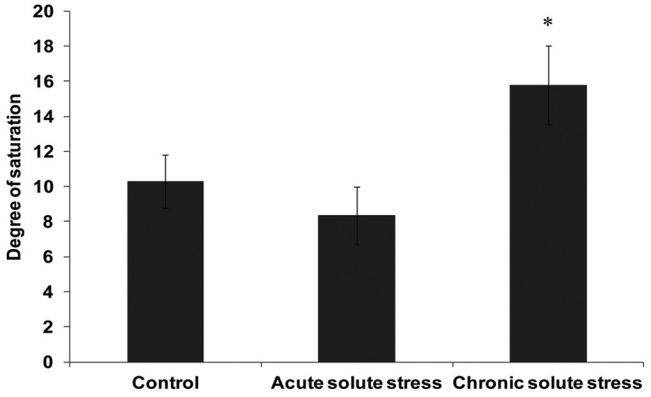

FIG 2 Degree of saturation of membrane fatty acids of *Sphingomonas* sp. LH128 biofilm cells grown in flow chambers without solute stress (control) and with acute or chronic solute stress. The values shown are the average of three biological replicates with the indicated standard deviations. The asterisk indicates a statistically significant difference from the control (*, $P < 0.05$).

plied in the biofilm systems. NaCl concentrations of 50 mM and higher resulted in increased lag phases and affected growth rate (Fig. 1), but at all salt concentrations, LH128 ultimately achieved an OD similar to that of nonstressed cultures. Cell size and morphology were not affected by NaCl, suggesting that the differences in OD_{600} were indeed due to differences in cell number (data not shown). Based on these results, a concentration of 450 mM NaCl that clearly affected LH128 growth (i.e., ca. 20% growth rate reduction in the exponential phase and increase in lag time to about 24 h) was selected for application in the biofilm systems. This concentration is slightly lower than that found in seawater (19) but was higher than that found in freshwater after deicing activities (33).

Effect of solute stress on LH128 biofilm structure. During the 11-day irrigation period, strain LH128 developed around 60-μm-thick biofilms under all conditions. Colonization occurred predominantly on and around the borders of the phenanthrene crystals. CLSM analysis revealed no visible structural differences between stressed and nonstressed biofilms, including biofilm horizontal and vertical cross-sections (see Fig. S2 in the supplemental material) and no significant differences in biovolume as a measure for biomass. Due to the heterogeneity and dispersed attachment of the biofilms to the phenanthrene crystals, no quantitative assessment of other biofilm parameters, such as roughness, could be obtained by image analysis.

Effect of solute stress on membrane fatty acids. The degree of cell membrane fatty acid saturation was significantly increased in chronic solute-stressed biofilms compared to nonstressed control biofilms ($P = 0.037$). Acute solute-stressed biofilms did not show significant differences compared to control biofilms (Fig. 2).

Effect of solute stress on phenanthrene degradation activity of biofilm cells. The effect of solute stress on phenanthrene degradation activity of the biofilm cells was measured in two ways. First, oxygen consumption in the flow chambers was measured by determining oxygen concentrations in the influent and effluent before and after solute stress. A significant reduction in the concentration of oxygen in the effluent medium compared to the influent medium was observed for inoculated flow chambers ($P = 0.001$), while no difference was recorded for uninoculated flow chambers (Fig. 3). This shows that the biofilm cells in the inoculated flow chambers were consuming oxygen and degrading phenanthrene. Oxygen consumption, however, did not significantly differ between control biofilms and acute ($P = 0.1$) or chronic ($P = 0.3$) solute-stressed biofilms (Fig. 3B). Second, the phenanthrene mineralization activity of biofilm cells recovered from the flow chambers was measured by determining the production of $^{14}CO_2$ from ^{14}C-labeled phenanthrene after 4 and 16 h of incubation (Fig. 4). Neither acute nor chronic solute stress-exposed cells showed a significant difference in $^{14}CO_2$ production compared to cells recovered from the control biofilm systems.

Gene expression analysis of biofilm cells. Both hierarchical clustering analysis and PCA of all microarray data showed strong clustering of the replicates for each condition with distinct clusters for each condition. Clusters of acute and chronic NaCl stressed biofilms were closer to each other than to the control biofilm cluster (data not shown). Of all targeted ORFs encoding putative proteins, 9% (656/7,033) and 12% (815/7,033) of the genes were differentially expressed in acute and chronic solute-stressed biofilms, respectively, compared to nonstressed biofilms (Table 1). Genes with increased expression were found less frequent than genes with decreased expression, i.e., 41% had increased expression upon acute and 45% upon chronic solute stress. In total, 4.6% (324/7,033) of the genes were differentially expressed as a response to both acute and chronic solute stress, with 2% having increased expression and 2.6% having decreased expression. About 30 and 40% of the genes with significantly altered expression upon acute and chronic solute stress, respectively, encoded hypothetical proteins or proteins with no known function.

Genes that were differentially expressed between stressed and nonstressed biofilms and which could be related to proteins with known function were classified into clusters of orthologous groups (COGs) (57) based on their predicted functions (Fig. 5). The majority of differentially expressed genes that could be associated with a putative function had reduced expression in response to both types of solute stress. Genes in the category of lipid transport and metabolism, as well as secondary metabolite transport and metabolism, had especially reduced expression as a response to acute solute stress, whereas genes in the category of DNA replication, recombination, and repair had increased ex-

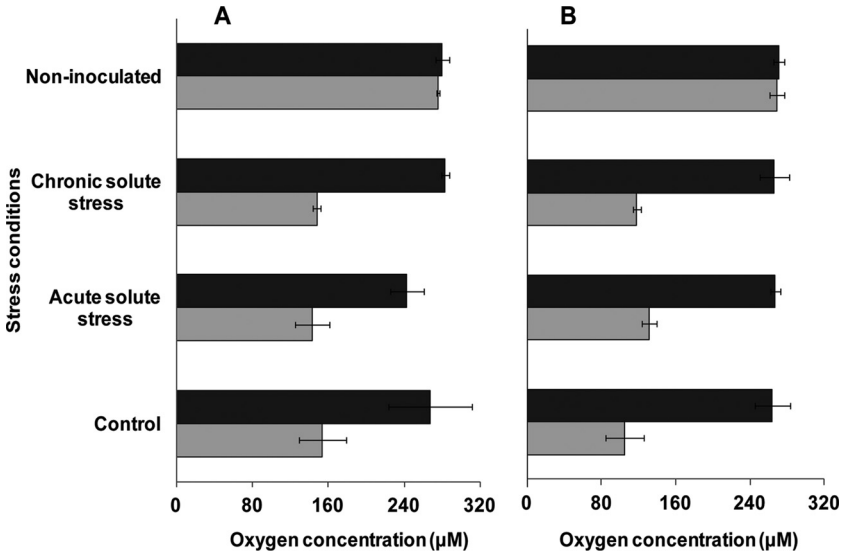

FIG 3 Oxygen concentrations in the influent and effluent of flow chambers colonized by *Sphingomonas* sp. LH128 biofilms and of noninoculated systems for comparison. The oxygen concentration was measured in the influent (black bars) and effluent (gray bars) before (A) and after (B) the application of solute stress in the inoculated systems. Values shown are the average of three biological replicates with the indicated standard deviations.

pression upon chronic solute stress. Only genes in the category of carbohydrate transport and metabolism had concomitant increased expression in response to acute and chronic solute stress. Genes in the category of translation, ribosomal structure, and signal transduction had reduced expression in both chronic and acute stress situations. A list of genes differentially expressed in each of the stress conditions compared to the control without stress is presented in Table S3 and Table S4 in the supplemental material. No differential expression of genes (see the list in Table S1 in the supplemental material) that are known to be involved in PAH degradation was observed as a response to both acute and chronic solute stress compared to nonstressed biofilms. In the following discussion, the major differentially expressed putative genes according to their COG classification are given.

(i) Amino acid transport and metabolism. Genes with increased expression in response to both acute and chronic solute stress included the cystathionine gamma-synthase (CGS)-encoding gene and genes involved in biosynthesis of glutamate, such as genes encoding formylglutamate amidohydrolase and ferredoxin-dependent glutamate synthase homologues. Genes with reduced expression as a response to both acute and chronic stress included genes encoding homologues of phosphoserine phosphatase,

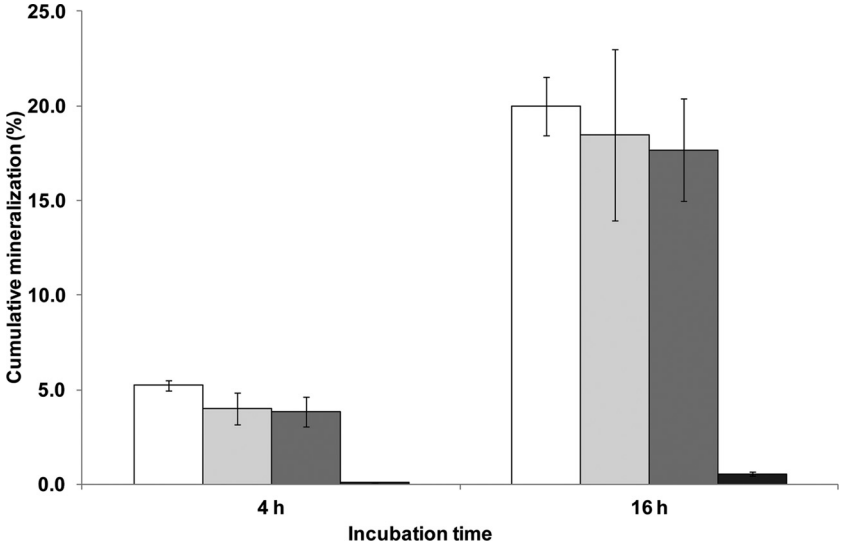

FIG 4 Phenanthrene mineralization activity of *Sphingomonas* sp. LH128 biofilm cells. Cells from control biofilms and from acute and chronic stressed biofilms were scraped and transferred to MM containing [^{14}C]phenanthrene and $^{14}CO_2$ production was measured after 4 and 16 h of incubation. Control condition without solute stress (white bars), acute NaCl stress condition (light gray bars), chronic NaCl stress condition (dark gray bars), and cell-free control condition (black bars). Values are expressed as the percentage of initial phenanthrene converted into CO_2 and are the average of three biological replicates, each of which was measured three times, with the indicated standard deviations ($n = 9$).

TABLE 1 Number of genes with increased and reduced expression (>2-fold changes) in *Sphingomonas* sp. LH128 biofilm under solute stress compared to nonstressed biofilms

Stress condition(s)	No. of differentially expressed genes		
	Increased expression	Reduced expression	Total
Acute solute stress	269	387	656
Chronic solute stress	368	447	815
Acute and chronic solute stress[a]	141	183	324

[a] That is, genes that were differentially expressed as a response to acute solute stress as well as chronic solute stress.

diaminopimelate/ornithine decarboxylase, and lysophospholipase L1-like esterase.

(ii) Carbohydrate transport and metabolism. Among the genes with increased expression in the category of carbohydrate transport and metabolism were putative osmoregulatory genes, including genes encoding homologues of proteins involved in the biosynthesis of trehalose, such as trehalose-6-phosphate synthase and trehalase, of the major facilitator superfamily MFS_1 proteins, and of fructose porters. Some genes, such as the Na^+/xyloside symporter and efflux-type transporter genes, were only induced as a response to chronic solute stress.

(iii) Transcriptional regulators and signal transductions. Among the major differentially expressed genes included in the transcriptional regulator and signal transduction category as a response to both acute and chronic solute stress were the genes encoding homologues of cold shock proteins and translation initiation factor IF-2. The majority of the genes involved in transcription, such as genes encoding homologues of the extracytoplasmic function (ECF) subfamily RNA polymerase sigma-24 factor and RNA polymerase factor sigma-54, showed reduced expression in response to both acute and chronic stress. Genes encoding homologues of the RNA polymerase sigma-70 factor and FecI-like sigma-24 had increased expression as a response to chronic solute stress.

(iv) Translational apparatus and ribosomal biogenesis. Genes in the translational apparatus and ribosomal biogenesis group are involved in controlling metabolically expensive protein expression. Most of the genes in these groups had reduced expression upon both acute and chronic solute stress. Genes with re-

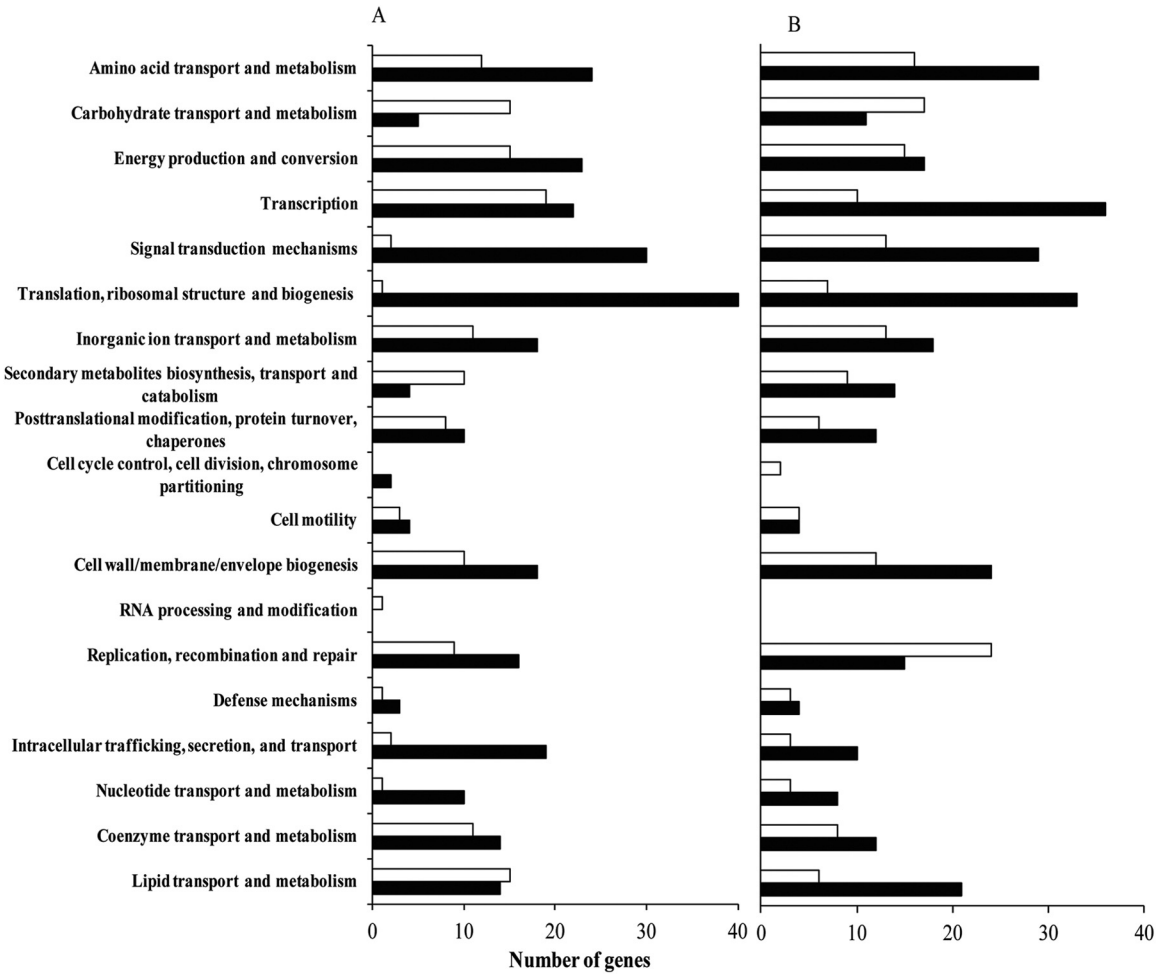

FIG 5 COG-based functional classification of differentially expressed genes in LH128 as a response to acute NaCl stress (A) and chronic NaCl stress (B) compared to control conditions. White bars indicate the number of genes with increased expression, while black bars indicate the number of genes with reduced expression. Genes classified in more than one category were counted more than once. Genes with unknown functions or encoding hypothetical proteins or classified in none of the mentioned categories were not included.

duced expression were mainly genes encoding ribosomal proteins, such as different 30S and 50S ribosomal proteins and elongation factors (Tu and Ts). The exception was ribosomal protein L4 that had increased expression during chronic solute stress.

(v) Ion transport and secondary metabolite biosynthesis. The ion transport and secondary metabolite biosynthesis category of genes includes several putative osmoregulatory and antioxidative stress response genes. The major known osmoregulatory genes with increased expression were the genes encoding ectoine synthase (45-fold increased expression) and ectoine hydroxylase (30-fold increased expression) homologues. Both were expressed in acute and chronic solute stressed biofilms. Other genes with increased expression as a response to both stress conditions were genes encoding homologues of cation/multidrug efflux pumps and of oxidative stress response proteins (catalase and oxidoreductase). Genes encoding a homologue of voltage gated Cl- channels (chloride channels) had increased expression only in case of acute solute stress. The gene encoding a putative NhaA-like Na^+/H^+ antiporter had increased expression upon chronic solute stress but reduced expression upon acute solute stress.

(vi) Posttranslational modification, protein turnover, and chaperones. Finally, genes associated with posttranslational modification, protein turnover, and chaperones, especially genes involved in cell protection against reactive oxygen species, had increased expression in response to both acute and chronic solute stress, including genes encoding a 1-Cys peroxiredoxin homologue, a putative redoxin domain-containing protein, and a glutathione *S*-transferase homologue. Genes encoding a molecular chaperone (small heat shock protein) and a disulfide bond (DSBA) oxidoreductase homologue had increased expression upon acute solute stress, and a gene encoding a homologue of the GrpE protein had reduced expression upon chronic solute stress.

(vii) Other categories. A number of genes belonging to other functional categories not mentioned above were differentially expressed in response to solute stress. Those included genes encoding homologues of proteins involved in genetic recombination, gene exchange, and cell motility. Genes involved in recombination and genetic exchange showed especially increased expression upon both acute and chronic stress exposure and included genes encoding homologues of resolvases, integrases, and transposases. Putative motility-associated genes showed decreased expression upon both stress conditions and included genes encoding homologues of flagellar proteins and proteins involved in chemotaxis. Other differentially expressed genes were a gene encoding an homologue of the rod shape-determining protein (RodA) that showed increased expression upon chronic stress and some genes encoding putative membrane bound protein such as genes encoding homologues of the small-conductance mechanosensitive channel (MSC), carbohydrate-selective porins, and porin B precursors (outer membrane glucose porin), which had increased expression upon both acute and chronic solute stress.

Confirmation of differential expression properties of selected genes by RT-qPCR. To validate the microarray data, the differential expression of nine selected ORFs was examined by RT-qPCR. These genes included six genes that showed increased expression and one gene that showed decreased expression. In addition, the expression of the gene encoding the PAH ring-hydroxylating dioxygenase α-subunit (*phnA1f*) and of *gfp* that was not differentially expressed in the microarray analysis was examined. The RT-qPCR data were in accordance with the microarray data with regard to the trends in differential expression for all of the selected genes (correlation coefficient of 0.74.), although differences in induction levels between microarray and RT-qPCR data were observed (see Fig. S3 in the supplemental material).

DISCUSSION

The aim of this study was to identify and compare the adaptive strategy and activity of *Sphingomonas* sp. LH128 biofilms in response to acute and chronic solute stress exposure. To the best of our knowledge, this is the first detailed transcriptomic study of biofilms of a PAH-degrading soil bacterium and *Sphingomonas* on solute stress in relation to its PAH-degrading activity. It should be noted that biofilms are complex in structure and are characterized by chemical gradients, which can result into the development of populations with different gene expression and physiological profiles within the biofilm structure (3). The physiological and transcriptomic data presented here should therefore be considered as values that are averaging potentially stratified biofilm gene expression. NaCl diffusion into and within the biofilm is expected to occur quite quickly (in about 3 min, the NaCl concentrations should be similar throughout the biofilm) as estimated based on theoretical assumptions of homogenous and monolayer biofilms (55). Consequently, NaCl concentrations are expected to be not different between upper and lower layers of the biofilms in both stress conditions. Such an overall approach of biofilm gene expression analysis has been reported for other bacteria, including *E. coli* (24), *Salmonella enterica* serovar Typhimurium (23), and *Pseudomonas aeruginosa* (60).

Despite the changes in the genome-wide expression, which clearly suggest an overall response to solute stress, no drastic changes in biofilm morphology were observed between control biofilms and NaCl stressed biofilms. Visual observation of the biofilm morphology showed that both stressed and nonstressed biofilms of LH128 colonized the flow chamber environment in a similar way, growing especially on and adjacent to the crystals, which is a colonization pattern that is in accordance with previous reports (63). A major physiological response on the NaCl stress was an increase in the degree of saturation of membrane fatty acids as a response to chronic solute stress. An increase in the relative abundance of saturated fatty acids has been proposed to reduce cell membrane fluidity and permeability and, as such, decrease the rate of water loss under osmotic stress (44). This has been shown in *S. wittichii* RW1 (38), where the ratio was increased by ~1.3-fold compared to an ~1.8-fold increase in LH128. The apparent lack of response of membrane fatty acid saturation to the acute solute stress could be explained by the fact that changes in membrane fatty acid saturation requires cell growth (26) and that the majority of the biofilm cells did not have time to grow during the 4-h exposure, with the doubling time of LH128 on phenanthrene being 11 h (P. Bruegelmans and D. Springael, unpublished results). This is in contrast with the clear response of the transcriptome on short solute stress. Cellular responses at the transcriptional level are, however, more rapid than at the membrane fatty acid level and do not require cell growth (11). Interestingly, no important changes in parameters related to *in situ* phenanthrene biodegradation activity, i.e., oxygen consumption and [^{14}C]phenanthrene mineralization activity were observed. Oxygen consumption can be related to phenanthrene degradation since phenanthrene was the only carbon source and no oxygen was consumed in chambers without phenanthrene. Oxygen is consumed in phenanthrene degradation

for respiration and for aromatic ring hydroxylation and ring cleavage reactions (42). The data suggest that the imposed stress conditions did not have a major impact on phenanthrene degradation and that the observed changes in transcriptome and membrane fatty acid saturation resulted in protection of the cells to solute stress without significant loss in phenanthrene degrading activity.

Both acute and chronic solute stress clearly affected the average transcriptome of the LH128 biofilm cells. It indeed shows that even in a short period of solute stress, the NaCl penetrated sufficiently deep into the biofilms to affect a substantial fraction of cells. The absence of differential expression of PAH catabolic genes agrees with the results inferred from the activity measurements and suggests that solute stress has no influence on the phenanthrene catalytic activity in biofilm systems at the transcription level. We have indications for phenanthrene inducible expression of at least *phnA1f* involved in initial aromatic ring hydroxylation (K. Wouters and D. Springael, unpublished results). Also, in salicylate-grown cells of *S. wittichii* RW1, the transcription of genes involved in aromatic degradation was not affected by immediate and long-term exposure to NaCl (38).

A variety of genes were differentially expressed which could be directly linked to osmotic and ionic stress release. One strategy used by strain LH128 appears to be the biosynthesis or accumulation of compatible solutes, e.g., amino acids such as glutamate, ectoine, and sugars such as trehalose. Glutamate is an important osmoregulatory amino acid in bacteria exposed to solute stress (13) and the expression of its biosynthesis genes upon solute exposure was also reported in *Sinorhizobium meliloti* (16). The importance of ectoine as an osmoprotectant response to solute stress was shown for *S. meliloti* and *Desulfovibrio vulgaris* (25, 34), while biosynthesis of trehalose as a response to NaCl stress was also suggested in *S. wittichii* RW1 (38). The role of import of compatible solutes is further accentuated by the increased expression of genes encoding proteins that show homology to permeases and conductance mechanosensitive channel (MSC). MSC is located in the cytoplasmic membrane and is responsible for the release and transport of various compounds during stress exposure and, as such, acts as a safety valve against the build-up of turgor pressure (29). Another set of genes that can be directly related to solute stress release are genes associated with ion homeostasis, such as a gene encoding an NahA Na^+/H^+ antiporter homologue. Na^+/H^+ antiporters extrude Na^+, which is toxic if accumulated in the cell, while importing H^+ to create a proton gradient (15, 56). Its increased expression upon chronic stress and not upon immediate solute stress indicates that Na^+ is tolerated initially to avoid osmotic stress but later extruded from the cytoplasm to mitigate ionic stress. Similar to observations in *D. vulgaris*, several homologues of cation/multidrug efflux pumps appear to be involved in the defense against ionic stress in LH128 under both acute and chronic solute stress (25). Other identified gene functions directly related with osmotic and ionic stress release was a chloride channel homologue and a RodA homologue. Chloride channels are involved in ion homeostasis, membrane potential stabilization, and cell volume regulation (35) and increased expression of this gene under solute stress was also observed in strain RW1 (38). RodA is involved in peptidoglycan biosynthesis and plays a role in cytoskeletal ring assembly and maintenance in different organisms such as *E. coli* (32).

Several genes were differentially expressed whose deduced functions could be related to a general stress response rather than to osmotic and ionic stress. A first set of such genes is associated with general protein synthesis such as genes encoding ribosomal proteins, which showed reduced expression with the exception of the L4 protein. Reduced expression of genes encoding ribosomal proteins as a response to salt stress has also been documented for *D. vulgaris* and *S. meliloti* (16, 25) and has been proposed as an energy-saving mechanism to shut down other protein synthesis for an increased expression of genes important for adaptation to solute stress. Ribosomal protein L4 stabilizes mRNA by inhibiting RNase E activity, and its increased expression under stress conditions in *E. coli* has been related to the protection of stress-responsive transcripts and elevated production of stress-induced proteins (58). Genes controlling oxidative stress also had increased expression under salt stress. Similar findings were obtained in other bacteria, including RW1 (10, 25, 38). Perturbations of the cell membrane or alterations in intracellular enzyme activities due to osmotic stress can cause aberrant electron flow from the electron transport chain or cellular redox enzymes to O_2, resulting in the production of reactive oxygen species (31).

A response to stress often also involves several transcriptional factors. This also accounted for LH128. Reduced expression of gene encoding RNA polymerase sigma factor 54, which is involved in transcription of genes required for nitrogen assimilation and fixation, dicarboxylic acid transport, and pilus formation (53), suggests that LH128 as a response to the salt stress shuts down specific gene functions. In contrast to RW1 (38) and other bacteria (16), the gene encoding the extracytoplasmic function (ECF) subfamily RNA polymerase sigma-24 factor, showed reduced expression. This was unexpected since such factors are part of the bacterial stress response regulon by activating transcription of genes encoding gene products involved in defense or repair processes as a response to external stress signals (47). The increased expression of housekeeping gene sigma factor σ^{70} upon chronic but not acute solute stress indicated that key genes important for the survival of LH128 are expressed after long exposure to salt stress (49). The transcriptome data further showed increased expression of several genes that encode proteins that allow cells to cope with incorrectly folded or denatured proteins. Small heat shock proteins are often expressed in stress situations and assist in protein stability, while the DSBA protein catalyzes disulfide bond formation during folding of secreted proteins (47). The GrpE protein prevents in *E. coli*, together with DnaK and DnaJ, the aggregation of stress-denatured proteins in response to hyperosmotic and heat shock stress (20).

In accordance with planktonic cells of other bacteria, including strain RW1 (14, 25, 38), LH128 biofilm cells shows reduced expression of genes putatively involved in motility as a response to acute and chronic salt stress. It is currently unknown why bacteria reduce motility as a response to salt stress, but Liu et al. (41) suggested that it helps *Shewanella oneidensis* MR1 to conserve energy for cellular export of Na^+ during NaCl exposure. Differences in the motility of LH128 were not observed in the presence of 450 mM NaCl compared to cells in the absence of NaCl when examined by microscopy or in soft agar assays (data not shown). However, the effects of NaCl on biofilm cells could be different from planktonic cells. For instance, increased expression of motility genes was observed in biofilm cells compared to planktonic cells of *S. enterica* (23) and *E. coli* K-12 (17) without stress exposure, which has been related to detachment of cells from mature biofilms for colonization of free niches (58). Motility in *Bacillus*

thuringiensis 407 biofilms has been related to the generation of pores to increase nutrient flux (30).

In conclusion, the observed changes in whole-genome expression and membrane fatty acids suggests that, as a reaction to immediate NaCl stress, where the cells are expected to lose water, LH128 biofilm cells respond by the production or uptake of osmoprotectants and the decrease in the biosynthesis of proteins. Upon longer NaCl stress, LH128 appears to reduce the fluidity of the membrane by increasing the saturation of fatty acid, to stabilize the expression of stress response genes, and to control ion homeostasis and energy-demanding gene expression, for instance, for motility. These mechanisms apparently contribute in the immediate and long-term sustainment of the PAH catabolic activity in strain LH128 biofilms during solute stress exposure. Due to its inherent and rapid adaptation to increased salt concentrations, LH128 and possibly other *Sphingomonas* strains can contribute to the natural attenuation and biodegradation of pollutants in polluted environments experiencing regular fluctuations in solute concentrations.

ACKNOWLEDGMENTS

This research was supported by the EC FP7 Framework KBBE project BACSIN (grant KBBE-211684) and Fonds voor Wetenschappelijk Onderzoek–Vlaanderen (FWO-Vlaanderen) research grants G.0229.07 and G.0371.06.

REFERENCES

1. **Aspedon A, Palmer K, Whiteley M.** 2006. Microarray analysis of the osmotic stress response in *Pseudomonas aeruginosa*. J. Bacteriol. **188**: 2721–2725.
2. **Bastiaens L, et al.** 2000. Isolation of adherent polycyclic aromatic hydrocarbon (PAH)-degrading bacteria using PAH-sorbing carriers. Appl. Environ. Microbiol. **66**:1834–1843.
3. **Beloin C, Ghigo JM.** 2005. Finding gene-expression patterns in bacterial biofilms. Trends Microbiol. **13**:16–19.
4. **Benjamini Y, Hochberg Y.** 1995. Controlling the false discovery rate: a practical and powerful approach to multiple testing. J. R. Stat. Soc. Ser. B Stat. Methodol. **57**:289–300.
5. **Besemer J, Borodovsky M.** 2005. GeneMark: web software for gene finding in prokaryotes, eukaryotes, and viruses. Nucleic Acids Res. **33**:W451–W454.
6. **Beveridge TJ, Makin SA, Kadurugamuwa JL, Li Z.** 1997. Interactions between biofilms and the environment. FEMS Microbiol. Rev. **20**:291–303.
7. **Bligh EG, Dyer WJ.** 1959. A rapid method of total lipid extraction and purification. Can. J. Biochem. Physiol. **37**:911–917.
8. **Brazma A, et al.** 2001. Minimum information about a microarray experiment (MIAME)—toward standards for microarray data. Nat. Genet. **29**: 365–371.
9. **Busse MD, Bottomley PJ.** 1989. Growth and nodulation responses of *Rhizobium meliloti* to water stress induced by permeating and nonpermeating solutes. Appl. Environ. Microbiol. **55**:2431–2436.
10. **Chang WS, Li X, Halverson LJ.** 2009. Influence of water limitation on endogenous oxidative stress and cell death within unsaturated *Pseudomonas putida* biofilms. Environ. Microbiol. **11**:1482–1492.
11. **Conway T, Schoolnik GK.** 2003. Microarray expression profiling: capturing a genome-wide portrait of the transcriptome. Mol. Microbiol. **47**: 879–889.
12. **Csonka LN.** 1989. Physiological and genetic responses of bacteria to osmotic stress. Microbiol. Rev. **53**:121–147.
13. **Csonka LN, Ikeda TP, Fletcher SA, Kustu S.** 1994. The accumulation of glutamate is necessary for optimal growth of *Salmonella typhimurium* in media of high osmolality but not induction of the *proU* operon. J. Bacteriol. **176**:6324–6333.
14. **Cytryn EJ, et al.** 2007. Transcriptional and physiological responses of *Bradyrhizobium japonicum* to desiccation-induced stress. J. Bacteriol. **189**: 6751–6762.
15. **Dibrov P.** 2005. The sodium cycle in *Vibrio cholerae*: riddles in the dark. Biochemistry (Mosc.) **70**:150–153.
16. **Dominguez-Ferreras A, et al.** 2006. Transcriptome profiling reveals the importance of plasmid pSymB for osmoadaptation of *Sinorhizobium meliloti*. J. Bacteriol. **188**:7617–7625.
17. **Domka J, Lee J, Bansal T, Wood TK.** 2007. Temporal gene-expression in *Escherichia coli* K-12 biofilms. Environ. Microbiol. **9**:332–346.
18. **Edgar R, Domrachev M, Lash AE.** 2002. Gene Expression Omnibus: NCBI gene expression and hybridization array data repository. Nucleic Acids Res. **30**:207–210.
19. **Emerson WH, Jamieson DT.** 1967. Some physical properties of sea water in various concentrations. Desalination **3**:213–224.
20. **Grimshaw JPA, Jelesarov I, Siegenthaler RK, Christen P.** 2003. Thermosensor action of GrpE. J. Biol. Chem. **278**:19048–19053.
21. **Hall-Stoodley L, Costerton JW, Stoodley P.** 2004. Bacterial biofilms: from the natural environment to infectious diseases. Nat. Rev. Microbiol. **2**:95–108.
22. **Halverson LJ, Firestone MK.** 2000. Differential effects of permeating and nonpermeating solutes on the fatty acid composition of *Pseudomonas putida*. Appl. Environ. Microbiol. **66**:2414–2421.
23. **Hamilton S, et al.** 2009. The transcriptional programme of *Salmonella enterica* serovar Typhimurium reveals a key role for tryptophan metabolism in biofilms. BMC Genomics **10**:599. doi:10.1186/1471-2164-10-599.
24. **Hancock V, Klemm P.** 2007. Global gene expression profiling of asymptomatic bacteriuria *Escherichia coli* during biofilm growth in human urine. Infect. Immun. **75**:966–976.
25. **He Z, et al.** 2010. Global transcriptional, physiological, and metabolite analyses of the responses of *Desulfovibrio vulgaris* Hildenborough to salt adaptation. Appl. Environ. Microbiol. **76**:1574–1586.
26. **Heipieper H, Neumann G, Cornelissen S, Meinhardt F.** 2007. Solvent-tolerant bacteria for biotransformations in two-phase fermentation systems. Appl. Microbiol. Biotechnol. **74**:961–973.
27. **Heipieper HJ, Meulenbeld G, van Oirschot Q, de Bont J.** 1996. Effect of environmental factors on the *trans/cis* ratio of unsaturated fatty acids in *Pseudomonas putida* S12. Appl. Environ. Microbiol. **62**:2773–2777.
28. **Heydorn A, et al.** 2000. Quantification of biofilm structures by the novel computer program Comstat. Microbiology **146**:2395–2407.
29. **Hoffmann T, Boiangiu C, Moses S, Bremer E.** 2008. Responses of *Bacillus subtilis* to hypotonic challenges: physiological contributions of mechanosensitive channels to cellular survival. Appl. Environ. Microbiol. **74**:2454–2460.
30. **Houry A, et al.** 2012. Bacterial swimmers that infiltrate and take over the biofilm matrix. Proc. Natl. Acad. Sci. U. S. A. **109**:13088–13093.
31. **Imlay JA.** 2003. Pathways of oxidative damage. Annu. Rev. Microbiol. **57**:395–418.
32. **Ishino F, et al.** 1986. Peptidoglycan synthetic activities in membranes of *Escherichia coli* caused by overproduction of penicillin-binding protein 2 and *rodA* protein. J. Biol. Chem. **261**:7024–7031.
33. **Jackson RB, Jobbäy EG.** 2005. From icy roads to salty streams. Proc. Natl. Acad. Sci. U. S. A. **102**:14487–14488.
34. **Jebbar M, Sohn-Basser L, Bremer E, Bernard T, Blanco C.** 2005. Ectoine-induced proteins in *Sinorhizobium meliloti* include an ectoine ABC-type transporter involved in osmoprotection and ectoine catabolism. J. Bacteriol. **187**:1293–1304.
35. **Jentsch TJ, Gunther W.** 1997. Chloride channels: an emerging molecular picture. Bioessays **19**:117–126.
36. **Johnsen AR, et al.** 2006. Microbial degradation of street dust polycyclic aromatic hydrocarbons in microcosms simulating diffuse pollution of urban soil. Environ. Microbiol. **8**:535–545.
37. **Johnsen AR, Wick LY, Harms H.** 2005. Principles of microbial PAH-degradation in soil. Environ. Pollut. **133**:71–84.
38. **Johnson D, Coronado E, Moreno-Forero S, Heipieper H, van der Meer J.** 2011. Transcriptome and membrane fatty acid analyses reveal different strategies for responding to permeating and non-permeating solutes in the bacterium *Sphingomonas wittichii*. BMC Microbiol. **11**:250. doi:10.1186/1471-2180-11-250.
39. **Leys NM, Ryngaert A, Bastiaens L, Verstraete W, Top EM, Springael D.** 2004. Occurrence and phylogenetic diversity of *Sphingomonas* strains in soils contaminated with polycyclic aromatic hydrocarbons. Appl. Environ. Microbiol. **70**:1944–1955.
40. **Liste H-H, Alexander M.** 2000. Plant-promoted pyrene degradation in soil. Chemosphere **40**:7–10.

41. **Liu Y, et al.** 2005. Transcriptome analysis of *Shewanella oneidensis* MR-1 in response to elevated salt conditions. J. Bacteriol. **187**:2501–2507.
42. **Mallick S, Chatterjee S, Dutta TK.** 2007. A novel degradation pathway in the assimilation of phenanthrene by *Staphylococcus* sp. strain PN/Y via meta-cleavage of 2-hydroxy-1-naphthoic acid: formation of *trans*-2,3-dioxo-5-(2-hydroxyphenyl)-pent-4-enoic acid. Microbiology **153**:2104–2115.
43. **Mantell A, Frenkel H, Meiri A.** 1985. Drip irrigation of cotton with saline-sodic water. Irrig. Sci. **6**:95–106.
44. **Mrozik A, Piotrowska-Seget Z, Labuzek S.** 2004. Cytoplasmatic bacterial membrane responses to environmental perturbations. Pol. J. Environ. Stud. **13**:487–494.
45. **Nordberg EK.** 2005. YODA: selecting signature oligonucleotides. Bioinformatics **21**:1365–1370.
46. **Papendick RI, Campbell GS.** 1980. Theory and measurement of water potential, p 1–22. *In* Parr JF, Gardner WR, Elliott LF (ed), Water potential relations in soil microbiology. Soil Science Society of America, Madison, WI.
47. **Raivio TL, Silhavy TJ.** 2001. Periplasmic stress and ECF sigma factors. Annu. Rev. Microbiol. **55**:591–624.
48. **Ramakrishna DM, Viraraghavan T.** 2005. Environmental impact of chemical deicers: a review. Water Air Soil Pollut. **166**:49–63.
49. **Ramos JL, Marques S, Timmis KN.** 1997. Transcriptional control of the *Pseudomonas* TOL plasmid catabolic operons is achieved through an interplay of host factors and plasmid-encoded regulators. Annu. Rev. Microbiol. **51**:341–373.
50. **Reasoner DJ, Geldreich EE.** 1985. A new medium for the enumeration and subculture of bacteria from potable water. Appl. Environ. Microbiol. **49**:1–7.
51. **Record MT, Jr, Courtenay ES, Cayley DS, Guttman HJ.** 1998. Responses of *Escherichia coli* to osmotic stress: large changes in amounts of cytoplasmic solutes and water. Trends Biochem. Sci. **23**:143–148.
52. **Shabala L, et al.** 2009. Ion transport and osmotic adjustment in *Escherichia coli* in response to ionic and non-ionic osmotica. Environ. Microbiol. **11**:137–148.
53. **Shingler V.** 1996. Signal sensing by sigma 54-dependent regulators: derepression as a control mechanism. Mol. Microbiol. **19**:409–416.
54. **Singh R, Paul D, Jain RK.** 2006. Biofilms: implications in bioremediation. Trends Microbiol. **14**:389–397.
55. **Stewart PS.** 2003. Diffusion in biofilms. J. Bacteriol. **185**:1485–1491.
56. **Taglicht D, Padan E, Schuldiner S.** 1991. Overproduction and purification of a functional Na^+/H^+ antiporter coded by *nhaA* (ant) from *Escherichia coli*. J. Biol. Chem. **266**:11289–11294.
57. **Tatusov RL, Koonin EV, Lipman DJ.** 1997. A genomic perspective on protein families. Science **278**:631–637.
58. **Tolker-Nielsen T, et al.** 2000. Development and dynamics of *Pseudomonas* sp. biofilms. J. Bacteriol. **182**:6482–6489.
59. **Uyttebroek M, Ortega-Calvo JJ, Breugelmans P, Springael D.** 2006. Comparison of mineralization of solid-sorbed phenanthrene by polycyclic aromatic hydrocarbon (PAH)-degrading *Mycobacterium* spp. and *Sphingomonas* spp. Appl. Microbiol. Biotechnol. **72**:829–836.
60. **Waite RD, Papakonstantinopoulou A, Littler E, Curtis MA.** 2005. Transcriptome analysis of *Pseudomonas aeruginosa* growth: comparison of gene expression in planktonic cultures and developing and mature biofilms. J. Bacteriol. **187**:6571–6576.
61. **Welsh DT.** 2000. Ecological significance of compatible solute accumulation by micro-organisms: from single cells to global climate. FEMS Microbiol. Rev. **24**:263–290.
62. **White DC, Sutton SD, Ringelberg DB.** 1996. The genus *Sphingomonas*: physiology and ecology. Curr. Opin. Biotechnol. **7**:301–306.
63. **Wouters K, et al.** 2010. A non-invasive fluorescent staining procedure allows confocal laser scanning microscopy based imaging of *Mycobacterium* in multispecies biofilms colonizing and degrading polycyclic aromatic hydrocarbons. J. Microbiol. Methods **83**:317–325.